

# Kitaev-Heisenberg Model on a Honeycomb Lattice: Possible Exotic Phases in Iridium Oxides $A_2\text{IrO}_3$

Jiří Chaloupka,<sup>1,2</sup> George Jackeli,<sup>2,\*</sup> and Giniyat Khaliullin<sup>2</sup>

<sup>1</sup>*Department of Condensed Matter Physics, Masaryk University, Kotlářská 2, 61137 Brno, Czech Republic*

<sup>2</sup>*Max-Planck-Institut für Festkörperforschung, Heisenbergstrasse 1, D-70569 Stuttgart, Germany*

(Dated: July 12, 2010)

We derive and study a spin one-half Hamiltonian on a honeycomb lattice describing the exchange interactions between  $\text{Ir}^{4+}$  ions in a family of layered iridates  $A_2\text{IrO}_3$  ( $A=\text{Li, Na}$ ). Depending on the microscopic parameters, the Hamiltonian interpolates between the Heisenberg and exactly solvable Kitaev models. Exact diagonalization and a complementary spin-wave analysis reveal the presence of an extended spin-liquid phase near the Kitaev limit and a conventional Néel state close to the Heisenberg limit. The two phases are separated by an unusual stripy antiferromagnetic state, which is the exact ground state of the model at the midpoint between two limits.

PACS numbers: 75.10.Jm, 75.25.Dk, 75.30.Et

Magnetic systems exhibit, most commonly, long-range classical order at sufficiently low temperatures. An exception are frustrated magnets, in which the topology of the underlying lattice and/or competing interactions lead to an extensively degenerate manifold of classical states. In such systems, exotic quantum phases of Mott insulators (spin liquids, valence bond solids, etc.) can emerge as the true ground states (for reviews see Refs. [1, 2]). In quantum spin liquids, strong zero-point fluctuations of correlated spins prevent them to “freeze” into magnetic or statically dimerized patterns, and conventional phase transitions that break time-reversal and lattice symmetries are avoided. Spin liquids have attracted particular attention since Anderson proposed their possible connection to superconductivity of cuprates [3].

Recently, spin-liquid states of matter have been exemplified, on a quantitative level, by an exactly solvable model by Kitaev [4]. His model deals with spins one-half that live on a honeycomb lattice. The nearest-neighbor (NN) spins interact in a simple Ising-like fashion but, because different bonds use different spin components [see Fig. 1(a)], the model is highly frustrated. Its ground state is spin-disordered and supports the emergent gapless excitations represented by Majorana fermions [4]. Spin-spin correlations are, however, short-ranged and confined to NN pairs [5, 6]. This may suggest the robustness of the disordered state to spin perturbations. Indeed, Tsvelik has shown [7] that there is a window of stability for the spin-liquid state in the Kitaev model perturbed by isotropic Heisenberg exchange.

Finding a physical realization of this remarkable model is a great challenge, also because of its special properties attractive for quantum computation [4]. As the key element of the model is a bond-selective spin anisotropy, one possible idea [8] is to explore Mott insulators of late transition metal ions with orbital degeneracy, in which the bond directional nature of electron orbitals can be translated into a desired anisotropy of magnetic interactions through strong spin-orbit coupling.

In this Letter, we examine the iridium oxides  $A_2\text{IrO}_3$  from this perspective. In these compounds, the  $\text{Ir}^{4+}$  ions have an effective spin one-half moment and form weakly coupled honeycomb-lattice planes. Our analysis of the underlying exchange mechanisms shows that the spin Hamiltonian comprises two terms, ferromagnetic (FM) and antiferromagnetic (AF), in the form of Kitaev and Heisenberg models, respectively. The model has an interesting phase behavior and hosts, in addition to the spin-liquid state, an unusual AF order that is also an exact solution at a certain point in phase space.

Experimental studies of iridium compounds are rather scarce, and the nature of their insulating behavior is not yet fully understood. In fact,  $\text{Na}_2\text{IrO}_3$  was suggested as an interesting candidate for a topological band insulator [9]. Given that high temperature magnetic susceptibilities of  $\text{Na}_2\text{IrO}_3$  and  $\text{Li}_2\text{IrO}_3$  obey the Curie-Weiss law with an effective moment corresponding  $S = 1/2$  per Ir ion [10–13], we start here with the Mott insulator picture.

*The Hamiltonian.*— We recall that the  $\text{Ir}^{4+}$  ion in the octahedral field has a single hole in the threefold degenerate  $t_{2g}$  level hosting an orbital angular momentum  $l = 1$ . Strong spin-orbit coupling lifts this degeneracy, and the resulting ground state is a Kramers doublet with total angular momentum one-half [14], referred to as “spin” hereafter. In fact, it is predominantly of orbital origin, and this is what makes the magnetic interactions highly anisotropic due to the spin-orbit entanglement of magnetic and real spaces. In  $A_2\text{IrO}_3$  compounds, the  $\text{IrO}_6$  octahedra share the edges, and Ir ions can communicate through two  $90^\circ$  Ir-O-Ir exchange paths [8] or via direct overlap of their orbitals. Collecting the possible exchange processes (discussed below) and projecting them onto the lowest Kramers doublet with  $S = 1/2$ , we obtain the following spin Hamiltonian on a given NN  $ij$  bond:

$$\mathcal{H}_{ij}^{(\gamma)} = -J_1 S_i^\gamma S_j^\gamma + J_2 \mathbf{S}_i \cdot \mathbf{S}_j . \quad (1)$$

Here, spin quantization axes are taken along the cubic axes of  $\text{IrO}_6$  octahedra. In a honeycomb lattice formed

by Ir ions, there are three distinct types of NN bonds referred to as  $\gamma (= x, y, z)$  bonds because they host the Ising-like  $J_1$  coupling between the  $\gamma$  components of spins [see Fig. 1(a)]. The first part of Eq. (1) is thus nothing but the FM Kitaev model, and the  $J_2$  term is a conventional AF Heisenberg model. The exchange constants  $J_1$  and  $J_2$  are derived from a multiorbital Hubbard Hamiltonian consisting of the local interactions and the hopping term. The latter describes  $t_{pd\pi}$  hopping between Ir  $5d$  and O  $2p$  orbitals via the charge-transfer gap  $\Delta_{pd}$ , and a direct  $dd$  overlap  $t'$  between NN Ir  $t_{2g}$  orbitals [15]. We find  $J_1 = (\eta_1 + 2\eta_2)$  and  $J_2 = (\eta_2 + \eta_3)$ . Hereafter, we use  $4t^2/9U_d$  as our energy unit, where  $t = t_{pd\pi}^2/\Delta_{pd}$ , and  $U_d$  stands for the Coulomb repulsion on the same  $d$  orbitals. There are three physically distinct virtual processes that determine the set of  $\eta$  parameters and thus the ratio  $J_2/J_1$ . The  $\eta_1 = \frac{6J_H}{U_d - 3J_H} \frac{U_d}{U_d - J_H}$  term appears due to the multiplet structure of the excited levels induced by Hund's coupling  $J_H$  [8]. The processes when two holes meet at the same oxygen site (and experience  $U_p$  repulsion) and when they are cyclically exchanged around a  $\text{Ir}_2\text{O}_2$  square plaquette bring together a  $\eta_2 = \frac{U_p}{\Delta_{pd} + U_p/2} \frac{U_d}{\Delta_{pd}}$  contribution. Further, a direct  $dd$ -hopping  $t'$  between NN Ir  $t_{2g}$  orbitals contributes to the Heisenberg term with exchange coupling  $\eta_3 = (t'/t)^2$ . It is difficult to estimate the values of all the parameters involved; however, we expect  $\eta_1$  to be the largest, of the order of 1, and  $\eta_{2,3} < 1$ .

We parametrize the exchange couplings as  $J_1 = 2\alpha$  and  $J_2 = 1 - \alpha$  and study the properties of Kitaev-Heisenberg model (1) in the whole parameter space  $0 \leq \alpha \leq 1$ .

*Phase diagram.*— At  $\alpha = 0$ , we are left with the Heisenberg model exhibiting the Néel order with a staggered moment reduced to  $\langle S^z \rangle \simeq 0.24$  [16]. The opposite limit,  $\alpha = 1$ , corresponds to the exactly solvable Kitaev model with a short-range spin-liquid state [4], where spin correlation functions are identically zero beyond the NN distance and, on a given NN bond, only the components of spins matching the bond type are correlated [5].

Interestingly, the model is exactly solvable at  $\alpha = \frac{1}{2}$ , too. At this point Eq. (1) reads, e.g., on a  $z$ -type bond, as  $\mathcal{H}_{ij}^{(z)} = \frac{1}{2}(S_i^x S_j^x + S_i^y S_j^y - S_i^z S_j^z)$ . This anisotropic Hamiltonian can be mapped to that of a simple Heisenberg model on all bonds simultaneously [17]. Specifically, we divide the honeycomb lattice into four sublattices [see Fig. 1(b)] and introduce the rotated operators  $\tilde{\mathbf{S}}$ : While  $\tilde{\mathbf{S}} = \mathbf{S}$  in one of the sublattices,  $\tilde{\mathbf{S}}$  on the remaining three sublattices differs from the original  $\mathbf{S}$  by the sign of two appropriate components, depending on the sublattice they belong to. In the new basis, Eq. (1) takes the form

$$\mathcal{H}_{ij}^{(\gamma)} = -2(2\alpha - 1) \tilde{S}_i^\gamma \tilde{S}_j^\gamma - (1 - \alpha) \tilde{\mathbf{S}}_i \cdot \tilde{\mathbf{S}}_j. \quad (2)$$

At  $\alpha = \frac{1}{2}$ , the first term vanishes and we obtain the isotropic, both in spin and real spaces, Heisenberg model  $\mathcal{H}_{ij}^{(\gamma)} = -\frac{1}{2} \tilde{\mathbf{S}}_i \cdot \tilde{\mathbf{S}}_j$  with FM coupling. Thus, at  $\alpha = \frac{1}{2}$ ,

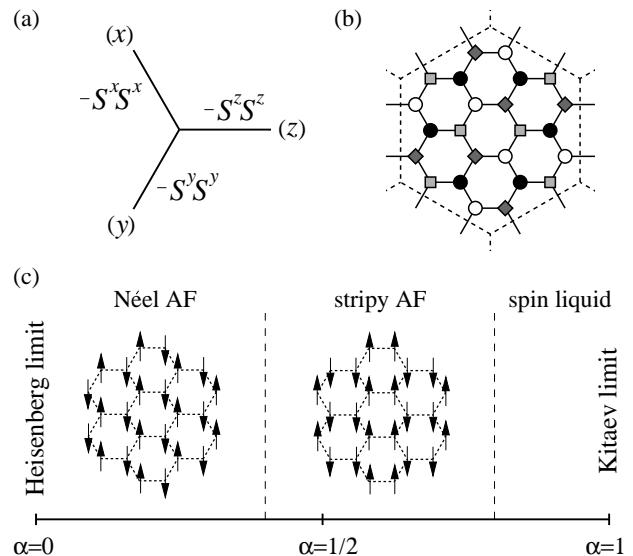


FIG. 1: (a) Three types of bonds in the honeycomb lattice and Kitaev part of the interaction. (b) The supercell of the four-sublattice system enabling the transformation of the model (1) into the Hamiltonian of a simple ferromagnet at  $\alpha = \frac{1}{2}$ . This supercell with periodic boundary conditions applied was used as a cluster for the exact diagonalization. (c) Schematic phase diagram: With increasing  $\alpha$ , the ground state changes from the Néel AF order to the stripy AF state (being a fluctuation-free exact solution at  $\alpha = \frac{1}{2}$ ) and to the Kitaev spin liquid. See the text for the critical values of  $\alpha$ .

i.e., at  $J_1 = 2J_2$ , the exact ground state of model (1) is a fully polarized FM state in the rotated basis. Now consider the FM array of spins with, e.g.,  $\langle \tilde{S}^z \rangle = 1/2$ , and map it back to the original spin basis. The resulting order corresponds to a stripy AF pattern of the original magnetic moments depicted in Fig. 1(c). Note that such a stripy order, despite being of AF type, is fluctuation-free at  $\alpha = \frac{1}{2}$  and would thus show a fully saturated AF order parameter.

The above discussion suggests three possible ground state phases of the model (1) as shown in Fig. 1(c): (i) Néel order near  $\alpha = 0$ , (ii) stripy AF order around  $\alpha = \frac{1}{2}$ , and (iii) a spin-liquid phase close to  $\alpha = 1$ .

We first consider the ordered phases. Except special cases of  $\alpha = 0$  and  $\alpha = \frac{1}{2}$  just discussed, the Hamiltonian (1) does not have any spin-rotational symmetry. However, a spurious  $SU(2)$  continuous symmetry and associated pseudo-Goldstone mode appear in a linear spin-wave (SW) description. As in the case of a similar model on a cubic lattice [18], we find that quantum fluctuations restore the underlying discrete (hexagonal) symmetry of the model, selecting thereby the direction of ordered moments along one of the cubic axes (of  $\text{IrO}_6$  octahedra), and also open a gap in SW spectra. Considering the quantum energy cost for rotating the order parameter by a small angle away from a cubic axis, we find a quantum SW gap  $\Delta \simeq \frac{2}{\alpha}(\alpha - \frac{1}{2})^2$  for  $\alpha \sim \frac{1}{2}$ .

The classical phase boundary between Néel and stripy AF orderings is at  $\alpha = \frac{1}{3}$ , where linear SW spectra of both states develop zero-energy lines [19], reflecting the infinite degeneracy of classical states. At  $\alpha = \frac{1}{3}$ , Eq. (1) reads, e.g., on  $z$ -type bonds, as  $\mathcal{H}_{ij}^{(z)} = \frac{2}{3}(S_i^x S_j^x + S_i^y S_j^y)$ ; i.e., only two spin components are coupled on a given bond. Considering Néel or stripy AF with ordered spins parallel to the  $z$  axis, one finds that flipping all the spins along a zig zag chain, formed by  $x$ - and  $y$ -type bonds, does not change classical energy. This degeneracy is again accidental (an artifact of classical treatment) and can thus be lifted by quantum fluctuations. They favor the Néel state and shift the classical phase boundary to a larger value  $\alpha \simeq 0.4$ . This estimate is obtained by comparing the energies of the Néel [ $e_1 \simeq -\frac{3}{16}(3-5\alpha)$ ] and the stripy [ $e_2 \simeq -\frac{1}{8}(5\alpha-3+\frac{1}{\alpha})$ ] states including quantum corrections via second-order perturbation theory and matches well the numerical result found below.

Now, we discuss the phase behavior at  $\frac{1}{2} < \alpha < 1$ , i.e., in between two exact solutions (stripy AF at  $\alpha = \frac{1}{2}$  and a Kitaev spin-liquid at  $\alpha = 1$ ). In terms of rotated spins, all the couplings are of FM nature in this region [see Eq. (2)]. Thus, the FM order (read stripy AF of the original spins) is the only possible magnetic phase here to compete with the spin-liquid state. Since the latter is stable against a weak Heisenberg-type perturbation [7], a critical value of  $\alpha$  for the spin order/disorder transition must be located at some point less than 1. We give its naive estimate based on the energetics of these two phases. The energy of the stripy AF state is given above. The *upper* boundary for the energy of spin-liquid state is given by the expectation value of Eq. (2) using the exact result  $\langle S_i^z S_j^z \rangle = 0.13$  at  $\alpha = 1$  [5]. As a result, we find the transition from stripy AF order to a spin liquid at  $\alpha \simeq 0.86$  (close to the numerical result below).

Single-magnon excitations fail to detect this transition (since, as said above, there is not any other competing magnetic state). As  $\alpha$  increases, the lower branch of the linear SW spectrum just gradually softens, to become completely flat in the limit of  $\alpha = 1$  where the classical ground state is extensively degenerate [20]. We therefore suspect that the instability responsible for the collapse of magnetic order resides in the two-magnon sector [21]. Leaving this subtle issue for a future work, we now turn to our numerical results, which describe the evolution of spin correlations across the entire phase diagram.

*Numerical study.*— We use the Lanczos exact diagonalization method to study a 24-site cluster [see Fig. 1(b)] with periodic boundary conditions. The cluster is compatible with the above discussed four-sublattice transformation of Eq. (1) into Eq. (2). This provides an exact reference point  $\alpha = 1/2$ , which is useful for the interpretation of numerical data shown in Figs. (2) and (3) in terms of the original as well as transformed spins.

Figure 2 clearly locates the two phase transitions. In particular, a pronounced maximum in the second deriva-

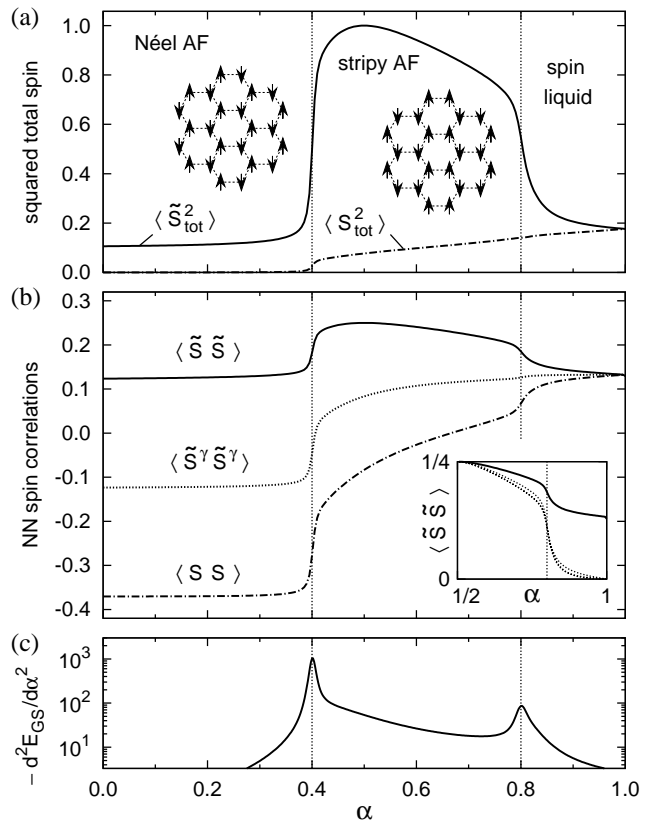


FIG. 2: (a) Squared total spin of the 24-site cluster, normalized to its value in the fully polarized FM state, as a function of  $\alpha$ . The solid (dot-dashed) line corresponds to the rotated (original) spin basis. (b) The NN spin correlations: The solid (dot-dashed) line corresponds to a scalar product of the rotated (original) spins. The component of the correlation function matching the bond direction is indicated by a dotted line. This quantity is the same in both bases. The inset compares NN spin correlations (solid line) above  $\alpha = 0.5$  with longer range spin correlations up to third-nearest neighbors (dotted lines). (c) Negatively taken second derivative of the ground state energy with respect to  $\alpha$ . Its maxima indicate the phase transitions at  $\alpha \simeq 0.4$  and  $0.8$ .

tive of the ground state energy [Fig. 2(c)] indicates a first-order transition from Néel to stripy AF phase at  $\alpha \simeq 0.4$ . The much weaker (note the *log* scale) and wider second peak at  $\alpha \simeq 0.8$  suggests a second- (or a weakly first-) order transition from stripy AF to a spin-liquid state.

Figure 2(a) shows the squared total spins  $\tilde{S}_{tot}^2$  and  $S_{tot}^2$  normalized to  $\tilde{S}(\tilde{S}+1)$  with  $\tilde{S} = N/2$  that can be reached in the FM state. Although these are not conserved quantities in the model, they characterize the phase map quite well. In particular, a long tail of  $\tilde{S}_{tot}^2$  above  $\alpha = 0.8$  indicates a “leakage” of stripy AF correlations into a spin-liquid phase. This is also evidenced by the behavior of longer range, beyond NN, spin correlations that are still visible in a spin-liquid regime, except close to the Kitaev limit where they vanish completely [see the inset in

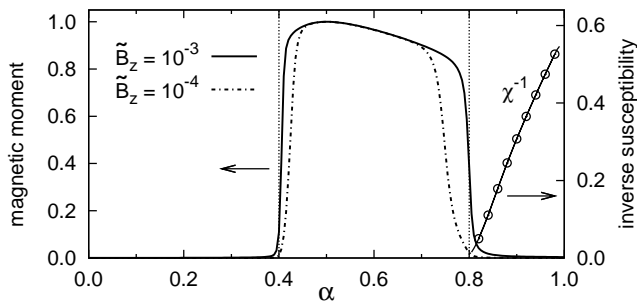


FIG. 3: Magnetic moment  $2\langle\tilde{S}_{\text{tot}}^z\rangle/N$  induced by field  $\tilde{B}_z$  (Zeeman coupled to the rotated spins). The circles at  $\alpha > 0.8$  show the inverse spin susceptibility to this field.

Fig. 2(b)].

Figure 2(b) highlights how the NN spin correlations evolve as their interactions change from one type to another. In the Néel state, where the model is more Heisenberg-like for the original spins, we reproduce  $\langle\mathbf{S}_i \cdot \mathbf{S}_j\rangle \simeq -0.37$  [16]. At the “hidden” FM Heisenberg point  $\alpha = 1/2$ , one finds  $\langle\tilde{\mathbf{S}}_i \cdot \tilde{\mathbf{S}}_j\rangle = \frac{1}{4}$ , equally contributed by all three components of the rotated spin  $\tilde{\mathbf{S}}$ . Things change dramatically in the spin-liquid phase: Here, a particular component of spin correlations  $\langle\tilde{S}_i^\gamma \tilde{S}_j^\gamma\rangle$ , dictated by the Kitaev model, dominates. Its value of 0.132 that we find at  $\alpha = 1$  agrees well with the exact result 0.131 for an infinite lattice [5].

Finally, we discuss the response to a weak magnetic field  $\tilde{B}^z$  which, in terms of original spins, linearly couples to the stripy AF order parameter. Figure 3 shows that even a very weak field induces a nearly saturated moment in the entire region of the stripy AF phase. As the system switches to the Néel phase, a response to the “stripy field”  $\tilde{B}^z$  drops abruptly to zero, as expected. The induced moment sharply reduces near  $\alpha = 0.8$ , too, but remains finite in a spin-liquid phase. Here the magnetization curve shows a linear dependence on  $\tilde{B}^z$ , and we may extract from its slope the susceptibility  $\chi = \langle\tilde{S}_{\text{tot}}^z\rangle/N\tilde{B}_z$ . Shown in Fig. 3 is the inverse value of  $\chi$  as a function of  $\alpha$ . This quantity scales with the energy gap between the ground state and the excited states that are accessible by the magnetic field. According to Kitaev’s solution [4], these states must belong to the flux sectors located at energies of the order of 1. The observed  $\chi^{-1} \propto (\alpha - 0.8)$  behavior shows that this characteristic (spin) gap gradually softens towards the  $\alpha \simeq 0.8$  critical point, as the spin correlations beyond the NN distances start to grow [see Fig. 2(b), inset].

Experimental data [10–13] are rather insufficient to conclusively locate the position of  $A_2\text{IrO}_3$  compounds in our phase diagram. Also, Na/Ir site disorder [13] has to be kept in mind: Often, nonmagnetic impurities induce local moments [22], and this has been shown to happen

in the Kitaev model as well [23].

In conclusion, we have examined the interactions and possible magnetic states in iridates  $A_2\text{IrO}_3$ . The obtained Kitaev-Heisenberg model shows rich behavior including a spin liquid and unusual stripy AF phases. We hope that these results will motivate experimental studies of layered iridates and similar compounds of late transition metal ions, where the physics of the Kitaev model might be within reach.

We thank B. Keimer, A. Schnyder, S. Trebst, and M. Zhitomirsky for discussions. We are grateful to H. Takagi and A.M. Tsvelik for valuable discussions and for communicating the unpublished results. Support from MSM0021622410 (J.C.) and GNSF/ST09-447 (G.J.) is acknowledged.

\* Also at Andronikashvili Institute of Physics, 0177 Tbilisi, Georgia.

- [1] L. Balents, *Nature (London)*, **464**, 199 (2010).
- [2] G. Misguich and C. Lhuillier, in *Frustrated Spin Systems*, edited by H.T. Diep (World Scientific, Singapore, 2005).
- [3] P.W. Anderson, *Science* **235**, 1196 (1987).
- [4] A. Kitaev, *Ann. Phys. (N.Y.)* **321**, 2 (2006).
- [5] G. Baskaran, S. Mandal, and R. Shankar, *Phys. Rev. Lett.* **98**, 247201 (2007).
- [6] H.-D. Chen and Z. Nussinov, *J. Phys. A* **41**, 075001 (2008).
- [7] A.M. Tsvelik, (unpublished).
- [8] G. Jackeli and G. Khaliullin, *Phys. Rev. Lett.* **102**, 017205 (2009).
- [9] A. Shitade *et al.*, *Phys. Rev. Lett.* **102**, 256403 (2009).
- [10] I. Felner and I.M. Bradarić, *Physica B* **311**, 195 (2002).
- [11] H. Kobayashi *et al.*, *J. Mater. Chem.* **13**, 957 (2003).
- [12] H. Takagi, (private communication).
- [13] Y. Singh and P. Gegenwart, arXiv:1003.0973.
- [14] B.J. Kim *et al.*, *Science* **323**, 1329 (2009).
- [15] On a  $\text{Ir}_2\text{O}_2$  plaquette, e.g., in the  $xy$  plane, the hopping term reads as  $-t_{pd}\pi p_{1(2),z}^\dagger(d_{i,xz(yz)} + d_{j,yz(xz)}) - t'd_{i,xy}^\dagger d_{j,xy} + h.c.$ , where  $p_{1(2),z}$  refers to a  $2p_z$  orbital of oxygen 1(2) shared by NN Ir ions  $i$  and  $j$ .
- [16] J.B. Fouet, P. Sindzingre, and C. Lhuillier, *Eur. Phys. J. B* **20**, 241 (2001).
- [17] G. Khaliullin, *Prog. Theor. Phys. Suppl.* **160**, 155 (2005).
- [18] G. Khaliullin, *Phys. Rev. B* **64**, 212405 (2001).
- [19] The details of SW analysis will be given elsewhere.
- [20] G. Baskaran, D. Sen, and R. Shankar, *Phys. Rev. B* **78**, 115116 (2008).
- [21] Preliminary calculations indicate that two-magnon bound states form at large  $\alpha$ . In case of the Kitaev toric code model, the relevance of multimagnon bound states to a quantum phase transition has been discussed by J. Vidal, R. Thomale, K.P. Schmidt, and S. Dusuel, *Phys. Rev. B* **80**, 081104(R) (2009).
- [22] G. Khaliullin, R. Kilian, S. Krivenko, and P. Fulde, *Phys. Rev. B* **56**, 11882 (1997).
- [23] A.J. Willans, J.T. Chalker, and R. Moessner, *Phys. Rev. Lett.* **104**, 237203 (2010).